J. Membrane Biol. 180, 205–212 (2001)
DOI: 10.1007/s002320010071

The Journal of
Membrane
Biology



# Plasma Membrane Protein Clusters Appear in CFTR-Expressing *Xenopus Laevis* Oocytes after cAMP Stimulation

**H. Schillers, T. Danker, M. Madeja, H. Oberleithner**
Department of Physiology, University Münster, Robert-Koch-Str. 27a, 48149 Münster, Germany

Received: 11 September 2000/Revised: 13 December 2000

**Abstract.** Membrane trafficking of the cystic fibrosis transmembrane conductance regulator (CFTR) is supposed to be an important mechanism controlled by the intracellular messenger cAMP. This has been shown with fluorescence techniques, electron microscopy and membrane capacitance measurements. In order to visualize protein insertion we applied atomic force microscopy (AFM) to inside-out oriented plasma membrane patches of CFTR-expressing *Xenopus laevis* oocytes before and after cAMP-stimulation. In a first step, oocytes injected with CFTR-cRNA were voltage-clamped, verifying successful CFTR expression. Water-injected oocytes served as controls. Then, plasma membrane patches were excised, placed (inside out) on glass and scanned by AFM. Before cAMP-stimulation plasma membranes of both water-injected and CFTR-expressing oocytes contained about 200 proteins per $\mu m^2$. Molecular protein masses were estimated from molecular volumes measured by AFM. Before cAMP-stimulation, protein distribution showed a peak value of 11 nm protein height corresponding to 475 kDa. During cAMP-stimulation with 1 mM isobutylmethylxanthine (IBMX) plasma membrane protein density increased in water-injected oocytes to 700 proteins per $\mu m^2$ while the peak value shifted to 7 nm protein height corresponding to 95 kDa. In contrast, CFTR-expressing oocytes showed after cAMP-stimulation about 400 proteins per $\mu m^2$ while protein distribution exhibited two peak values, one peak at 10 nm protein height corresponding to 275 kDa and another one at 14 nm corresponding to 750 kDa. They could represent heteromeric protein clusters associated with CFTR. In conclusion, we visualized plasma membrane protein insertion upon cAMP-stimulation and quantified protein distribution with AFM at molecular level. We propose that CFTR causes clustering of plasma membrane proteins.

**Keywords:** Membrane capacitance — Atomic force microscopy — Membrane trafficking — Chloride channel — Protein distribution

## Introduction

Formation of clusters as structural and functional units of proteins has been shown for numerous plasma membrane proteins, e.g., for $K_{ATP}$ channels containing four subunits of the inwardly rectifying $K^+$ channel family (Kir6.2) and four regulatory sulphonylurea receptor subunits (SUR1 and SUR2A/B) of the ATP-binding cassette (ABC) transporter family (Seino S, 1999). Cluster formation is necessary to obtain the full functionality of the channel. The cystic fibrosis transmembrane conductance regulator (CFTR), a member of the ABC-transporter family, is assumed to form clusters with different proteins in order to perform autocrine cell regulation. According to this hypothesis, CFTR allows ATP transport to the apical cell membrane surface, resulting in locally high ATP-concentrations (al-Awqati, 1995). In turn, extracellular ATP acts upon purinergic receptors that, via G-proteins, regulate phospholipase activities and plasma membrane ion channels (al-Awqati, 1995). However, such a mechanism is only feasible if the structural components of ATP-release and purinergic receptor function occur in a close spatial arrangement, since fast reduction of local ATP-concentration by 5′-nucleotidase activity and dilution effects would compromise such an autocrine mechanism.

For understanding the mechanisms of cluster formation it is important to know whether CFTR is a protein persistently located in the plasma membrane or whether CFTR is usually an intracellularly stored protein that

*Correspondence to:* H. Schillers

undergoes cAMP-controlled membrane trafficking. Cyclic AMP-controlled membrane trafficking of CFTR is controversially discussed at the moment. Some investigations show that cAMP-dependent protein kinase (PKA) stimulates trafficking of CFTR from intracellular pools to the plasma membrane while endocytotic retrieval of CFTR is simultaneously inhibited (Prince et al., 1993, 1994; Schwiebert et al., 1994; Takahashi et al., 1994; Howard et al., 1995; Tousson et al., 1996; Lukacs et al., 1997; Lehrich et al., 1998; Morris et al., 1998; Weber et al., 1999; Prince et al., 2000). In contrast, other investigators report that CFTR trafficking from intracellular compartments to the plasma membrane is not a major regulatory step in mediating CFTR function but rather assume that CFTR chloride channels, persistently present in the plasma membrane, are directly activated by cAMP-dependent PKA (Cheng et al., 1991; Tabcharani et al., 1991; Denning et al., 1992; Hug et al., 1997; Moyer et al., 1998).

Over the past years AFM was increasingly used to visualize cell surface structures and surface dynamics (Hoh and Hansma, 1992; Radmacher et al., 1992; Yang et al., 1993; Hansma and Hoh, 1994; Le Grimellec et al., 1994; Beckmann et al., 1998; Henderson and Oberleithner, 2000). AFM was recently used to show ATP-release to the surface of epithelial cells expressing CFTR (Schneider et al., 1999).

The present study addresses CFTR-associated cluster formation with AFM. We used the AFM to image the cytoplasmic surface of native plasma membranes of CFTR-positive and CFTR-negative *Xenopus laevis* oocytes before and after cAMP stimulation. Although trafficking of CFTR has been carefully examined by electrophysiological and fluorescence microscopy techniques (Moyer et al., 1998), little is known about the spatial distribution of this protein within the plasma membrane. AFM is a surface probe that visualizes protein structures at nanometer range in native membranes without using fixatives. This allows protein counting and protein height measurements essential for the determination of individual molecular masses and protein distribution on the cell surface.

## Materials and Methods

### Oocytes and cRNA Microinjection

Experiments were performed in *Xenopus laevis* oocytes, stage V, obtained as described (Madeja et al., 1991) and stored in Barth medium (in mM: 87 NaCl, 1 KCl, 1.5 $CaCl_2$, 0.8 $MgSO_4$, 2.4 $NaHCO_3$, 5 HEPES, pH 7.4 containing 100 IU/ml penicilline and 100 μg/ml streptomycine). The cDNA encoding human CFTR in pBluescript pBSSK$^-$ vector was kindly provided by R. Schreiber and K. Kunzelmann (Dept. of Physiology, University of Sydney, Australia). 5′capped cRNA was synthesized from KpnI linearized cDNA using T3 polymerase (Cap scribe T3, Boehringer, Mannheim). Oocytes were injected with 5 ng CFTR-cRNA dissolved in 50 nl double-distilled water and then stored at 19°C.

### Voltage-Clamp Experiments

Voltage-clamp analysis was performed 3 days after injection using a procedure described by Madeja et al. (1991). Oocytes were impaled with two electrodes (Hilgenberg, Malsfeld, Germany), each filled with 2.7 M KCl resulting in a resistance of 1 MΩ for the voltage electrode and 0.5 MΩ for the current electrode. Membrane currents were measured at clamped oocyte (holding potential −25 mV) plasma membrane voltages (Turbo TEC-03, npi, Tamm, Germany), in steps of 10 mV (range: −60 to +40 mV) and with 1000 ms duration. Current data were lowpass-filtered at 1 kHz (902, Frequency devices), and for data acquisition a pClamp 8 system (Axon Instruments, Foster City, CA, USA) was used. Voltage-clamp experiments were performed in ND96 buffer (in mM: 96 NaCl, 2 KCl, 1.8 $CaCl_2$, 1 $MgCl_2$, 5 HEPES, 2.5 Na-pyruvate, pH 7.4). For stimulation, 1 mM IBMX (3-isobutyl-1-methylxanthine, Sigma) was added.

CFTR-expressing oocytes identified by IBMX-inducible currents and water-injected oocytes (controls) were defolliculated by 1 hr treatment with 1 mg/ml collagenase (type D, Boehringer Mannheim). Then, oocytes rested for 2 hr in Barth medium. Vitelline membranes of oocytes were stripped after 10 min of hypertonic shrinkage in potassium aspartate buffer (in mM: 200 K-Aspartate, 20 KCl, 1 $MgCl_2$, 10 EGTA, 10 HEPES, pH 7.4).

### Plasma Membrane Preparation

CELLocate® glass cover slips (Eppendorf, Hamburg, Germany) containing lithographic grids (line to line distance: 55 μm) for membrane patch localization were cleaned by 1 hr treatment with concentrated $H_2SO_4$/30% $H_2O_2$ (9:1 v/v), rinsed three times with $ddH_2O$ and two times with acetone. 40 μl of an aqueous solution of poly-L-lysine (0.01% w/v, Sigma) was applied for 10 min to the clean side of each cover slip, then rinsed and finally baked for 1 hr at 60°C.

After removal of the vitelline membrane, oocytes were incubated for 6 min in Barth-Medium containing 1 mM IBMX and 0.1 μM FM1-43 (Molecular Probes, Eugene/OR, USA), a lipophilic fluorescence marker for plasma membrane staining. The oocyte was rinsed with Barth medium two times (removal of unused FM1-43), transiently attached to the coated glass cover slip (1 min) and then gently removed. The plasma membrane patch remaining on the glass surface was rinsed with $ddH_2O$, dried on air and located by fluorescence microscopy (excitation wavelength for FM1-43: 488 nm).

### Atomic Force Microscopy

AFM was performed in contact mode in air using a Nanoscope III Multimode-AFM (Digital Instruments, Santa Barbara, California, USA) with an E-type scanner (maximal scan area: 15 × 15 μM). Cellocates® were attached to stainless steel punches with double-sided adhesive tape and mounted in the commercially available fluid cell (Digital Instruments). V-shaped oxide-sharpened cantilevers with spring constants of 0.06 N/m (Digital Instruments) were used for scanning. Images (512 × 512 pixels) were captured with scan sizes between 1 and 25 $\mu m^2$ at a scan rate of 12 Hz (12 scan lines/sec) and loading forces less than 1 nN. Images were processed using the Nanoscope III software (Digital Instruments). Particle counting and 3D presentation were performed with the software SPIP (Scanning probe image processor, Image Metrology, Lyngby, Denmark). This software allows analysis of particles located close to each other through the determi-

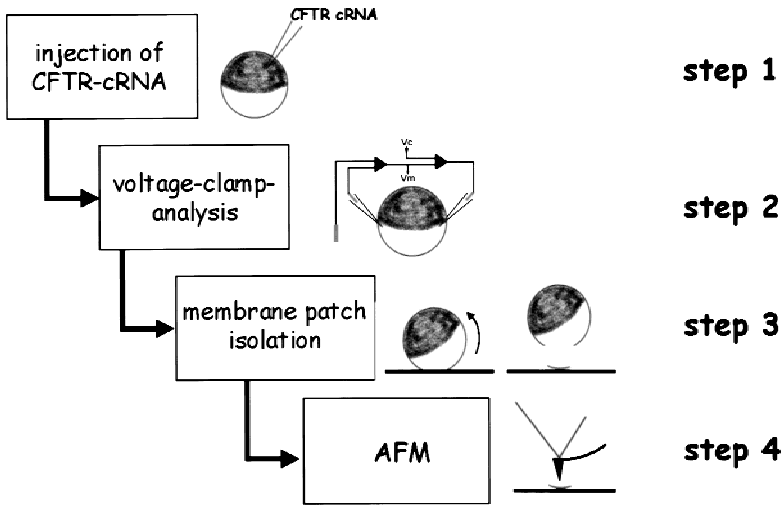


**Fig. 1.** Scheme of the experimental procedure. After injection of CFTR cRNA the expression of CFTR was examined with voltage-clamp experiments. Only membranes of oocytes which exhibited the expected currents in voltage-clamp analysis were isolated and scanned by AFM.

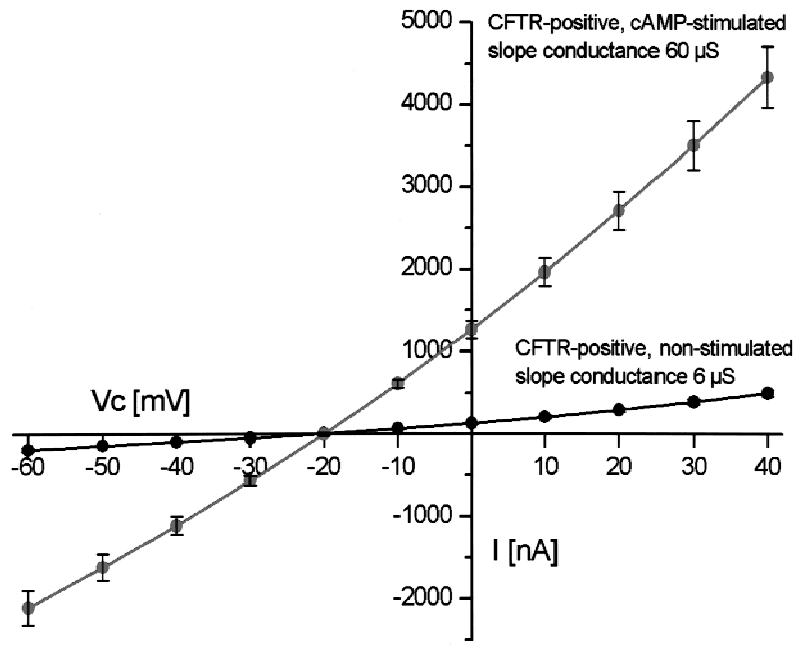


**Fig. 2.** Current-voltage relationships obtained in CFTR-positive oocytes (mean ± SEM, $n = 15$). Under non-stimulated conditions and following exposure of the oocytes to IBMX (1 mM) for 6 minutes. Voltage-clamp experiments were performed in ND96 buffer (in mM: 96 NaCl, 2 KCl, 1.8 $CaCl_2$, 1 $MgCl_2$, 5 HEPES, 2.5 Na-pyruvate, pH 7.4)

nation of "local minima" in height and therefore allows the definition of particle boundaries even from tightly packed structures. The precision of this process is affected by assignment of a threshold.

### Molecular Volume of Membrane Proteins

In order to estimate the molecular mass ($M_0$) of individual membrane proteins we used a model published previously (Lärmer et al., 1997). The calculation is based on a simplified model imaging a membrane protein as a sphere embedded in the lipid bilayer. The volume of a single protein ($V_{Prot}$) was calculated using the sphere's volume equation ($V = 4/3\ \pi\ r^3$), with the protein radius, $r$, given by the half height of the protein. The molecular mass $M_0$ can then be calculated:

$$M_0 = \frac{N_A}{V_1 + d \cdot V_2} \cdot V_{Prot}$$

In this equation $N_A$ is the Avogadro constant ($6.022 \times 10^{23}$ mol$^{-1}$), $V_1$ is the partial specific volume of the protein (0.74 cm$^3$/g), $V_2$ is the specific volume of water (1 cm$^3$/g) and $d$ is a factor describing the extent of hydration for air-dried proteins (0.4 mol $H_2O$/mol protein). This method was successfully used also by other researchers (Pietrasanta et al., 1999). Treatment of the membrane with trypsin (0.05% in PBS) for 1 min shows that the structures are protease-digestible and thus identified as proteins (Schillers et al., 2000).

## Results

We used *Xenopus laevis* oocytes as expression system for human CFTR. Three days after injection of CFTR-cRNA we examined the expression of CFTR with voltage-clamp experiments. Only membranes of oocytes exhibiting

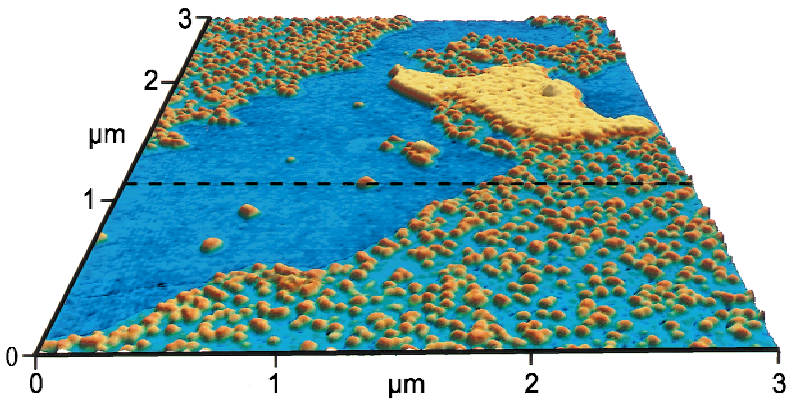


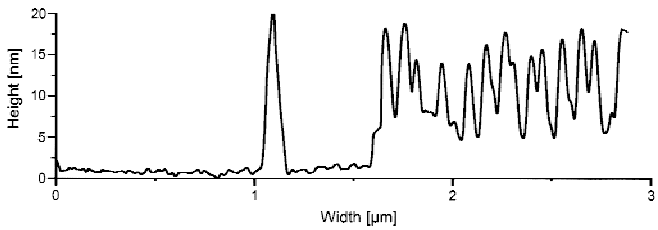


**Fig. 3.** Color-coded view of a 9 $\mu m^2$ scan area containing plasma membrane fragments attached to the poly-L-lysine-coated glass surface. Poly-L-lysine-coated glass is shown in "blue", the lipid bilayer membrane is shown in "turquoise", the membrane proteins are shown in "brown" and yet unidentified intracellular material is shown in "bright yellow". The broken line in the upper part of Fig. 3 corresponds to the profile line in the lower part showing the lipid bilayer with a height of about 5 nm. Proteins protrude from the inner surface of the plasma membrane with a height up to 20 nm.

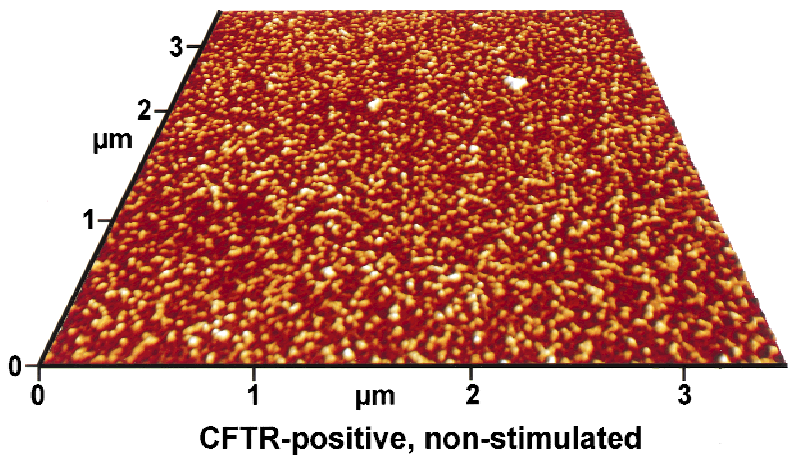


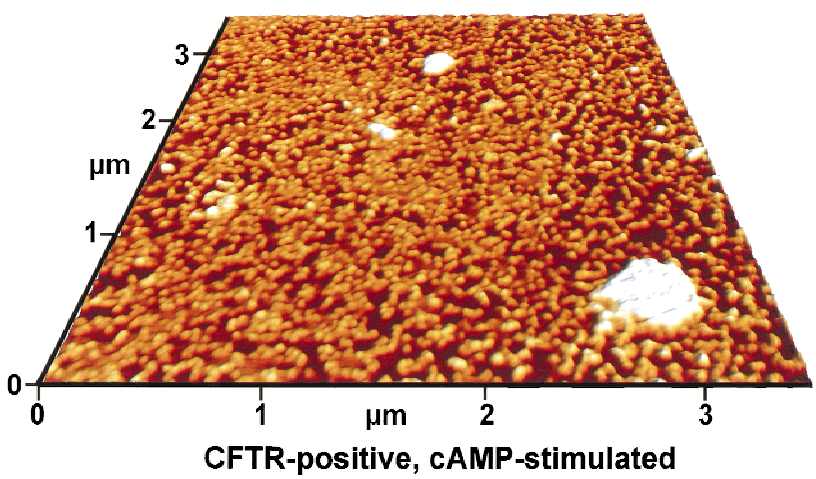


**Fig. 4.** Membrane patches of CFTR-positive oocytes. The membrane patch shown in the upper part of Fig. 4 was isolated before cAMP stimulation, the membrane shown in the lower part of Fig. 4 was isolated during cAMP-stimulation. In this color-coded view the plasma membrane, 5 nm in height, is shown in "brown". Proteins are shown with a color gradient from dark yellow to white, corresponding to heights from 6–20 nm. The large white spots are yet unidentified intracellular structures.

IBMX-inducible currents in voltage-clamp analysis were isolated and scanned by AFM. This experimental procedure ensures that the plasma membrane investigated by AFM contains functional CFTR. The step by step protocol applied in this study is shown in Fig. 1. It leads from functional expression of CFTR down to structural identification of plasma membrane protein clusters associated with CFTR. Electrical characterization indicates a slope conductance for non-stimulated CFTR-positive oocytes of about 6 μS, increasing up to 60 μS after 6 min of incubation with 1 mM IBMX (Fig. 2). This indicates a voltage-current relationship typical for CFTR-expressing oocytes (Cunningham et al., 1992; Mall et al., 1996).

Atomic force microscopy revealed large patches of inside-out oriented plasma membrane, areas without membrane and small regions with relatively high structures, probably intracellular material (e.g., yolk proteins). Edges of membrane were used to determine total height of plasma membrane and its protruding structures. Figure 3 shows a 3D color-coded view of a 9 $\mu m^2$ scan area containing plasma membrane fragments attached to the poly-L-lysine coated glass surface and some intracellular material. Poly-L-lysine-coated glass is shown in "blue", the lipid bilayer membrane is shown in "turquoise", the membrane proteins are shown in "brown" and the intracellular material is shown in "bright yellow". Membrane fragmentation occurs frequently due to the preparation method we used. The broken line in the upper part of Fig. 3 corresponds to the profile line in the lower part showing the lipid bilayer with a height of about 5 nm. Proteins protrude from the inner surface of the plasma membrane with heights up to 20 nm. Proteins appear with different heights and shapes. Some proteins are located so close to each other that they overlap or merge into one structure. In Fig. 3 we used this specific color-coding to emphasize the height differences between glass and membrane. This led to a poorer contrast for small protein structures. In Fig. 4 we focused on the protein structures and thus used a different color coding.

Figure 4 shows two 12.25 $\mu m^2$ membrane areas of CFTR-positive oocytes. The membrane patch shown in the upper part of Fig. 4 was isolated before cAMP stimulation, the membrane shown in the lower part of Fig. 4 was isolated during cAMP-stimulation. In this 3D color-coded view the plasma membrane, 5 nm in height, is shown in "brown". Proteins are shown with a color gradient from dark yellow to white, corresponding to heights from 6 nm to 20 nm. The proteins differ from each other in height and shape. Some are hardly detectable, others are up to 20 nm in height. The apparent shape of the proteins is found usually to be conical, most likely due to the fact that lateral dimensions of the base of individual proteins are overestimated as a result of AFM-tip geometry (Lärmer et al., 1997). Some proteins apparently exhibit "shoulders", while others stand so close to each other that they overlap. The main difference between cAMP-stimulated and non-stimulated oocyte membranes is the protein density. Quantification of protein distribution is shown in Fig. 5. Molecular volumes were estimated from protein heights measured by AFM. Molecular weights were then calculated from the respective volume measurements (Schneider et al., 1998) (for details see Materials and Methods). Each data set was obtained from four oocytes (three patches of 4 $\mu m^2$ per oocyte). A mean density of 200 proteins per $\mu m^2$ in non-stimulated CFTR-positive and control (water-injected = CFTR-negative) oocyte membrane was found. The hatched area in Fig. 5 represents the respec-

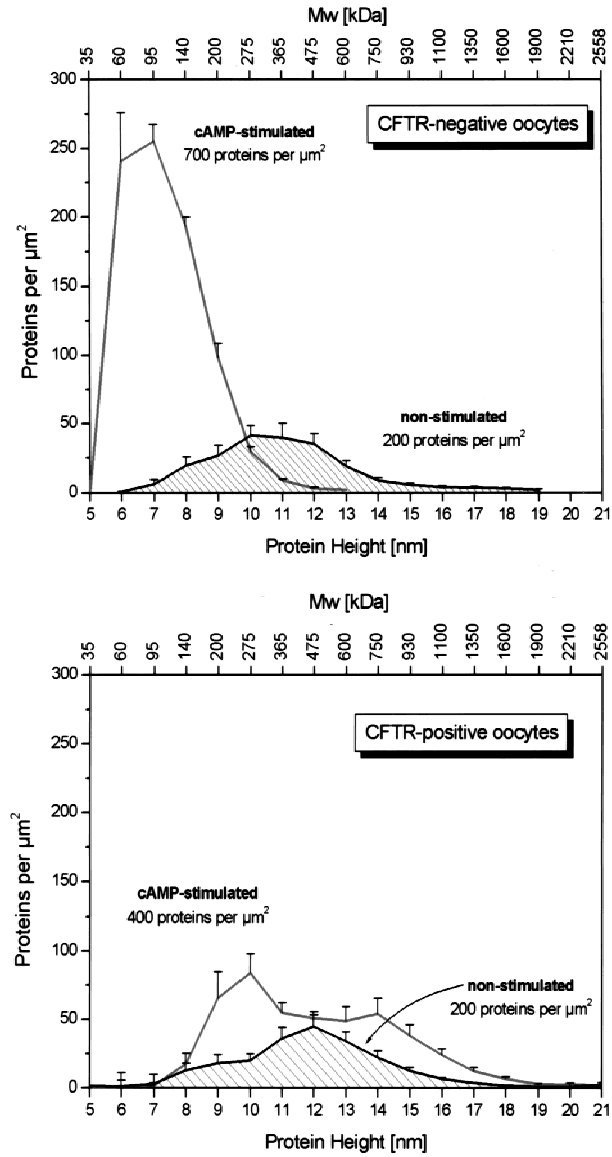


**Fig. 5.** Protein distribution of CFTR-negative (upper part of Fig. 5) and CFTR-positive (lower part of Fig. 5) plasma membrane (mean ± SEM, $n = 12$; 4 oocytes, 3 patches per oocyte). The hatched areas represent the respective height distributions of non-stimulated oocytes.

**Table.** Protein densities and molecular masses in plasma membrane of *Xenopus laevis* before and during cAMP-stimulation estimated by atomic force microscopy

| Preparation | CFTR-negative oocyte | | CFTR-positive oocyte | |
|---|---|---|---|---|
| Condition | nonstimulated | cAMP-stimulated | nonstimulated | cAMP-stimulated |
| Density; proteins per $\mu m^2$ | 200 | 700 | 200 | 400 |
| Molecular mass; mean value | 379 kDa | 165 kDa | 442 kDa | 464 kDa |
| Molecular mass; peak value | 275 kDa | 95 kDa | 475 kDa | 275 kDa and 750 kDa |

tive height distribution. Average plasma membrane protein height of CFTR-negative oocytes is 11.1 nm, corresponding to a molecular mass of 379 kDa with a peak value of 10 nm, corresponding to a molecular mass of 275 kDa (Fig. 5, upper part and Table). CFTR-positive oocytes show an average protein height of 11.7 nm, corresponding to molecular mass of 442 kDa with a peak value of 12 nm, corresponding to a molecular mass of 475 kDa (Fig. 5, lower part and Table). The differences in protein distribution between CFTR-negative and CFTR-positive oocytes before stimulation are small. Stimulation with IBMX dramatically changes protein distribution in both CFTR-negative and CFTR-positive oocytes. Density of small proteins increases in membranes of water-injected oocytes from 200 to 700 proteins per $\mu m^2$ with an average height of 8.4 nm, corresponding to a molecular mass of 165 kDa and a sharp peak value at 7 nm, corresponding to a molecular mass of 95 kDa (Fig. 5, upper part and Table). In membranes of CFTR-positive oocytes the protein density increases in response to IBMX from 200 to 400 proteins per $\mu m^2$ with an average protein height of 11.8 nm, corresponding to a molecular mass of 464 kDa. Protein distribution shows two peak values, at 10 nm and at 14 nm, corresponding to molecular masses of 275 kDa and 750 kDa, respectively (Fig. 5, lower part and Table).

## Discussion

We observed and quantified the cAMP-induced change in protein distribution and protein density in a native plasma membrane. Measurements were based on protein height since vertical resolution of the AFM is better than 0.5 nm (Henderson & Oberleithner, 2000). Three observations could be made: (*i*) a difference in protein distribution between CFTR-negative and CFTR-positive oocytes without cAMP stimulation, (*ii*) a cAMP-induced shift of protein distribution towards small proteins in CFTR-negative oocytes, (*iii*) a cAMP-induced double-peak distribution of membrane proteins in CFTR-positive oocytes.

We have not yet succeeded in specifically identifying the structures visualized on the cytoplasmic cell surface but argue that the differences observed between CFTR-negative and CFTR-positive oocytes are caused by CFTR. Protrusions emerging from the lipid membrane towards the cytoplasmic space are proteins since they disappear upon trypsin treatment as shown previously (Schillers et al., 2000).

We estimated the molecular masses of individual membrane proteins/protein clusters according to a model published previously (Lärmer et al., 1997). The calculation is based on a simplified model imaging a membrane protein as a sphere embedded in the lipid bilayer. This model has been proved useful also for calculating molecular masses of isolated proteins imaged by AFM (Schneider et al., 1998; Pietrasanta et al., 1999).

### Difference in Protein Distribution between CFTR-negative Oocytes and CFTR-positive Oocytes without cAMP-Stimulation

We found virtually no difference in the total number of proteins per $\mu m^2$ for CFTR-negative and CFTR-positive oocytes. Area covered by proteins can be calculated from the histograms of Fig. 5. The data indicate that without cAMP-stimulation CFTR-positive oocytes show 20% more protein covered area as compared to CFTR-negative oocytes. CFTR-negative oocytes show a rather broad dispersion of protein heights, whereas CFTR-positive oocytes exhibit a prominent protein population with a height of 12 nm corresponding to 475 kDa.

We assume that this protein population is most likely a protein multimere rather than a single protein. The molecular weight of mature glycosylated CFTR is 180 kDa (Moyer et al., 1998) corresponding to a height of 8.7 nm. Therefore, the peak value of 475 kDa, as found in nonstimulated CFTR-positive oocytes, is unlikely to represent individual CFTR molecules. Nevertheless, the peak at 475 kDa is caused by CFTR. We assume that the large proteins represent multimeric clusters containing CFTR. The two mechanisms of CFTR-activation (cAMP-induced CFTR insertion into the plasma membrane and cAMP-induced activation of dormant CFTR in the plasma membrane) are mutually not exclusive. It has been reported that both mechanisms of CFTR activation can simultaneously take place in oocytes (Weber et al., 1999). Taken together, we assume

that the plasma membrane protein structure with an estimated molecular mass of 475 kDa is a CFTR-associated cluster.

### Sharp cAMP-induced Shift of Protein Distribution towards Small Proteins in Water-injected Oocytes

Cyclic AMP-stimulation increased protein density in plasma membrane in both CFTR-negative and CFTR-positive oocytes. However, in contrast to CFTR-positive oocytes, the plasma membrane of CFTR-negative oocytes exhibited a sharp peak in protein distribution at small molecular weight proteins. Recently it was shown that plasma membrane capacitance, a quantitative measure for lipid bilayer membrane insertion, increases during cAMP-induced exocytosis in CFTR-positive oocytes (Weber et al., 1999) and Chinese hamster ovary cells (Hug et al., 1997) but, interestingly, not in CFTR-negative cells. The number of proteins smaller than about 100 kDa may have been underestimated because the resolution is limited by the size of an individual pixel. With a scan size of 3.5 × 3.5 μm, each pixel has a lateral dimension of 7 × 7 nm. Currently we have no explanation for this phenomenon. A possible explanation for this apparent discrepancy in CFTR-negative cells—dramatic increase in protein density per unit membrane area (suggesting protein insertion through vesicle insertion) but no change in membrane capacitance (expected to occur when membrane is inserted)—could be that cAMP induces insertion of small vesicles with high protein density in the vesicle membrane. Then, the increase of membrane capacitance could be expected to be immeasurably small during cAMP-induced vesicle fusion while proteins occur at high densities in the plasma membrane.

Cyclic AMP-stimulation increased plasma membrane protein density considerably more in CFTR-negative oocytes as compared to CFTR-positive oocytes. This is most likely due to the fact that CFTR is indeed a protein in charge of cluster formation with other proteins. CFTR expression and membrane insertion leads to cluster formation with neighbouring proteins. This reduces the number of small proteins in the membrane while simultaneously raising the number of large protein clusters. However, we can not exclude the possibility that the increase in density of small proteins was due to dissociation of large multimers induced by cAMP.

### Cyclic AMP-induced Double-Peak Distribution of Membrane Proteins in CFTR-expressing Oocytes

The data obtained in CFTR-positive oocytes indicate that the protein-covered area increases in response to cAMP by about 110%. This observation strongly suggests protein insertion into the plasma membrane. While CFTR-negative oocytes exhibited upon cAMP-stimulation a new peak at 95 kDa with a simultaneous decrease in large proteins, CFTR-positive oocytes show two new peaks at 275 kDa and 750 kDa. Since both peaks do not appear in CFTR-negative oocytes in response to cAMP-stimulation, we conclude that the two peaks are caused by CFTR. Considering the molecular mass of 180 kDa for a CFTR monomer, the peak at 275 kDa and 750 kDa could be multimeric CFTR or CFTR forming clusters with other proteins. Dimerization of CFTR, as derived from electrical experiments, has been reported recently (Zerhusen et al., 1999). However, we want to emphasize that this is still a hypothesis because we have not yet identified individual CFTR molecules by AFM.

Taken together, the data show that upon stimulation with cAMP, CFTR is inserted into the plasma membrane, indicated by a shift in protein density and protein distribution. Insertion of CFTR into the plasma membrane leads to the formation of clusters, heteromeric structures composed of CFTR and other proteins with yet unknown stoichiometry.

We thank Drs. K. Kunzelman and R. Schreiber for the generous gift of cDNA encoding human CFTR in pBluescript pBSSK$^-$ vector. We gratefully acknowledge the technical assistance of Mrs. H. Arnold and thank all other collaborators in our laboratory involved in membrane transport for numerous discussions during the course of the experiments. The study was supported by the "Interdisziplinäres Zentrum für Klinische Forschung", IZKF.

## References

al-Awqati, Q. 1995. Regulation of ion channels by ABC transporters that secrete ATP. Science **269:**805–806

Beckmann, M., Nollert, P., and Kolb, H.A. 1998. Manipulation and molecular resolution of a phosphatidylcholine-supported planar bilayer by atomic force microscopy. *J. Membrane Biol.* **161:**227–233

Cheng, S.H., Rich, D.P., Marshall, J., Gregory, R.J., Welsh, M.J., and Smith, A.E. 1991. Phosphorylation of the R domain by cAMP-dependent protein kinase regulates the CFTR chloride channel. *Cell* **66:**1027–1036

Cunningham, S.A., Worrell, R.T., Benos, D.J., and Frizzell, R.A. 1992. cAMP-stimulated ion currents in *Xenopus* oocytes expressing CFTR cRNA. *Am. J. Physiol.* **262:**C783–C788

Denning, G.M., Ostedgaard, L.S., Cheng, S.H., Smith, A.E., and Welsh, M.J. 1992. Localization of cystic fibrosis transmembrane conductance regulator in chloride secretory epithelia. *J. Clin. Invest.* **89:**339–349

Hansma, H.G. and Hoh, J.H. 1994. Biomolecular imaging with the atomic force microscope. *Annu. Rev. Biophys. Biomol. Struct.* **23:**115–139

Henderson, R.M. and Oberleithner, H. 2000. Pushing, pulling, dragging, and vibrating renal epithelia by using atomic force microscopy. *Am. J. Physiol.* **278:**F689–F701

Hoh, J.H. and Hansma, P.K. 1992. Atomic force microscopy for high-resolution imaging in cell biology. *Trends Cell Biol.* **2:**208–213

Howard, M., DuVall, M.D., Devor, D.C., Dong, J.Y., Henze, K., and

Frizzell, R.A. 1995. Epitope tagging permits cell surface detection of functional CFTR. *Am. J. Physiol.* **269:**C1565–C1576

Hug, M.J., Thiele, I.E., and Greger, R. 1997. The role of exocytosis in the activation of the chloride conductance in Chinese hamster ovary cells (CHO) stably expressing CFTR. *Pflugers Arch.* **434:**779–784

Lärmer, J., Schneider, S.W., Danker, T., Schwab, A., and Oberleithner, H. 1997. Imaging excised apical plasma membrane patches of MDCK cells in physiological conditions with atomic force microscopy. *Pflugers Arch.* **434:**254–260

Le Grimellec, C., Lesniewska, E., Cachia, C., Schreiber, J.P., de Fornel, F., and Goudonnet, J.P. 1994. Imaging of the membrane surface of MDCK cells by atomic force microscopy. *Biophys. J.* **67:**36–41

Lehrich, R.W., Aller, S.G., Webster, P., Marino, C.R., and Forrest, J.N., Jr. 1998. Vasoactive intestinal peptide, forskolin, and genistein increase apical CFTR trafficking in the rectal gland of the spiny dogfish, *Squalus acanthias.* Acute regulation of CFTR trafficking in an intact epithelium. *J. Clin. Invest.* **101:**737–745

Lukacs, G.L., Segal, G., Kartner, N., Grinstein, S., Zhang, F. 1997. Constitutive internalization of cystic fibrosis transmembrane conductance regulator occurs via clathrin-dependent endocytosis und is regulated by protein phosphorylation. *Biochem. J.* **328:**353–361

Madeja, M., Musshoff, U., Kuhlmann, D., and Speckmann, E.J. 1991. Membrane currents elicited by the epileptogenic drug pentylenetetrazole in the native oocyte of *Xenopus laevis. Brain Res.* **553:**27–32

Mall, M., Hipper, A., Greger, R., and Kunzelmann, K. 1996. Wild type but not delta F508 CFTR inhibits $Na^+$ conductance when coexpressed in *Xenopus* oocytes. *FEBS Lett.* **381:**47–52

Morris, R.G., Tousson, A., Benos, D.J., and Schafer, J.A. 1998. Microtubule disruption inhibits AVT-stimulated $Cl^-$ secretion but not $Na^+$ reabsorption in A6 cells. *Am. J. Physiol.* **274:**F300–F314

Moyer, B. D., Loffing, J., Schwiebert, E.M., Loffing-Cueni, D., Halpin, P.A., Karlson, K.H., Ismailov, I.I., Guggino, W.B., Langford, G.M., and Stanton, B.A. 1998. Membrane trafficking of the cystic fibrosis gene product, cystic fibrosis transmembrane conductance regulator, tagged with green fluorescent protein in madin-darby canine kidney cells. *J. Biol. Chem.* **273:**21759–21768

Peters, K.W., Qi, J., Watkins, S.C., and Frizzell, R.A. 2000. Mechanisms underlying regulated CFTR trafficking. *Med. Clin. North Am.* **84:**633

Pietrasanta, L.I., Thrower, D., Hsieh, W., Rao, S., Stemmann, O., Lechner, J., Carbon, J., and Hansma, H. 1999. Probing the *Saccharomyces cerevisiae* centromeric DNA (CEN DNA)-binding factor 3 (CBF3) kinetochore complex by using atomic force microscopy. *Proc. Nat. Acad. Sci. USA* **96:**3757–3762

Prince, L.S., Tousson, A., and Marchase, R.B. 1993. Cell surface labeling of CFTR in T84 cells. *Am. J. Physiol.* **264:**C491–C498

Prince, L.S., Workman, R.B., Jr., and Marchase, R.B. 1994. Rapid endocytosis of the cystic fibrosis transmembrane conductance regulator chloride channel. *Proc. Nat. Acad. Sci. USA* **91:**5192–5196

Radmacher, M., Tillmann, R. W., Fritz, M., and Gaub, H. E. 1992. From molecules to cells: imaging soft samples with the atomic force microscope. *Science* **257:**1900–1905

Schillers, H., Danker, T., Schnittler, H., Lang, F., and Oberleithner, H. 2000. Plasma membrane plasticity of *Xenopus laevis* oocyte imaged with atomic force microscopy. *Cell Physiol. Biochem.* **10:**99–107

Schneider, S.W., Egan, M.E., Jena, B.P., Guggino, W.B., Oberleithner, H., and Geibel, J.P. 1999. Continuous detection of extracellular ATP on living cells by using atomic force microscopy. *Proc. Nat. Acad. Sci. USA* **96:**12180–12185

Schneider, S.W., Lärmer, J., Henderson, R.M., and Oberleithner, H. 1998. Molecular weights of individual proteins correlate with molecular volumes measured by atomic force microscopy. *Pflugers Arch.* **435:**362–367

Schwiebert, E.M., Gesek, F., Ercolani, L., Wjasow, C., Gruenert, D.C., Karlson, K., and Stanton, B.A. 1994. Heterotrimeric G proteins, vesicle trafficking, and CFTR $Cl^-$ channels. *Am. J. Physiol.* **267:**C272–C281

Seino, S. 1999. ATP-sensitive potassium channels: a model of heteromultimeric potassium channel/receptor assemblies. *Annu. Rev. Physiol.* **61:**337–362

Tabcharani, J.A., Chang, X.B., Riordan, J.R., and Hanrahan, J.W. 1991. Phosphorylation-regulated $Cl^-$ channel in CHO cells stably expressing the cystic fibrosis gene. *Nature* **352:**628–631

Takahashi, T., Matsushita, K., Welsh, M.J., and Stokes, J.B. 1994. Effect of cAMP on intracellular and extracellular ATP content of $Cl^-$-secreting epithelia and 3T3 fibroblasts. *J. Biol. Chem.* **269:**17853–17857

Tousson, A., Fuller, C.M., and Benos, D.J. 1996. Apical recruitment of CFTR in T-84 cells is dependent on cAMP and microtubules but not $Ca^{2+}$ or microfilaments. *J. Cell Sci.* **109:**1325–1334

Weber, W. M., Cuppens, H., Cassiman, J.J., Clauss, W., and Van Driessche, W. 1999. Capacitance measurements reveal different pathways for the activation of CFTR. *Pflugers Arch.* **438:**561–569

Yang, J., Tamm, L.K., Somlyo, A.P., and Shao, Z. 1993. Promises and problems of biological atomic force microscopy. *J. Microsc.* **171:**183–198

Zerhusen, B., Zhao, J., Xie, J., Davis, P. B., and Ma, J. 1999. A single conductance pore for chloride ions formed by two cystic fibrosis transmembrane conductance regulator molecules. *J. Biol. Chem.* **274:**7627–7630